Journal of Biochemistry and Biophysics
Volume 4 | Issue 1
ISSN: 2576-7623

Review Article Open Access

Statistical Characterization of Positive and Negative Ionospheric Storm Effects Using TEC and ROTI During Intense Geomagnetic Storms (2023–2026): An Article Review

Gebre Kalute Gebino[1*], Efrem Amanuel Data[2], Tegegn Teferi Agago[1], Bonaya Galma Elema[3]

[1]Department of Physics, Wolaita Sodo University, Wolaita Sodo, Ethiopia
[2]Department of Geology, Wolaita Sodo University, Wolaita Sodo, Ethiopia
[3]Department of Physics, Borana University, Yabello, Ethiopia

Corresponding Author: Gebre Kalute, Department of Physics, Wolaita Sodo University, Wolaita Sodo, Ethiopia,
E-mail: gebrekaluteg@gmail.com

Citation: Gebre Kalute Gebino, Efrem Amanuel Data, Tegegn Teferi Agago, Bonaya Galma Elema (2026) Statistical Characterization of Positive and Negative Ionospheric Storm Effects Using TEC and ROTI During Intense Geomagnetic Storms (2023–2026): An Article Review, J Biochem Biophy 4(1): 104

Received Date: July 25, 2026 **Accepted Date:** August 06, 2026 **Published Date:** August 10, 2026

Abstract

Intense geomagnetic storms perturb the ionosphere via a cascade of electrodynamic and thermospheric processes that are observed as both enhancements (positive storm effects) and depletions (negative storm effects) of Total Electron Content (TEC) and short-scale plasma structuring observed through the Rate of TEC Index (ROTI). The period 2023-2026 was the rising and maximum phase of Solar Cycle 25, during which a rare succession of powerful and extreme storms occurred, most prominently the 10-11 May 2024 storm, widely reported as the strongest geomagnetic disturbance in nearly two decades, and following storms in October 2024 and in 2025. In this review, we compile results of recent GNSS-, ionosonde- and satellite-based studies of the storm-time TEC and ROTI behaviour over equatorial, low-, middle- and high-latitude sectors. It examines the physical drivers of positive and negative ionospheric storm effects (prompt penetration electric fields, disturbance dynamo electric fields, neutral composition changes and travelling ionospheric disturbances) and assesses how recent statistical and classification frameworks have attempted to systematize storm-to-storm and region-to-region variability. The review identifies continuing gaps including the limited number of studies that statistically pool multiple storms across full solar cycle phases, inconsistent storm classification criteria, and uneven regional data coverage, particularly across Africa and the South Atlantic Anomaly. The review was concluded by outlining a statistical framework for characterizing positive and negative storm effects using combined TEC and ROTI metrics across the 2023–2026 storm catalogue, intended to guide future observational and modelling studies.

Keywords: ionospheric storm effects; Total Electron Content (TEC); Rate of TEC Index (ROTI); geomagnetic storms; Solar Cycle 25; GNSS; equatorial ionization anomaly; space weather

1. Introduction

Geomagnetic storms continue to be one of the most disruptive space weather phenomena of the Earth's ionosphere, with direct impacts on the Global Navigation Satellite System (GNSS) positioning, high-frequency communication, and satellite operations [1,6]. It is driven by solar wind magnetosphere interactions, can significantly disturb the ionosphere, altering electron density and degrading satellite-based communication and navigation systems [2].

Storm-time ionospheric disturbances are typically classified as positive storm effects, which are characterized by increases in TEC and electron density relative to quiet-time levels, or negative storm effects, which are characterized by decreases in TEC and electron density [3]. Both types of disturbances may be observed in sequence at a single location as a storm evolves through its main and recovery phases. In addition to these large-scale TEC changes, storms also produce small-scale plasma irregularities, which are conveniently quantified by the Rate of TEC Index (ROTI) that captures short-period fluctuations associated with scintillation-producing structures. The April 2023 superstorm lets us to have a unique opportunity to analyze large-scale TEC perturbations [7].

The ascending phase and the peak of Solar Cycle 25, which covers the years 2023 to 2026, has already witnessed a much greater frequency of intense and extreme geomagnetic storms than the moderate Solar Cycle 24 that preceded it. The storm of 10–11 May 2024, associated with a SYM-H minimum of about −518 nT [19] and a Dst minimum of about −412 to −410 nT [12,16], has been identified as the most significant geomagnetic disturbance in nearly two [11], and it produced ionospheric responses that were documented on nearly every continent, from super-fountain effect enhancements over the American and Pacific sectors [19] to widespread positioning outages for high-accuracy GNSS users [18]. Subsequent storms in October 2024 [11] and through 2025 [9] have added further case studies characterizing the equatorial ionization anomaly (EIA), disturbance dynamo effects, and irregularity occurrence during the solar maximum interval.

There are three objectives of the review. First, it reviews the physical mechanisms responsible for the positive and negative TEC storm effects and for the irregularities detected by ROTI. Second, it reviews recent (2023-2026) observational studies in latitudinal sectors, outlining methodological approaches and main findings. Third, it reviews the current statistical and classification frameworks for characterizing storm impacts across multiple events [5], and the research gap that necessitates a specific statistical characterization study for the 2023–2026 storm periods.

2. Physical Mechanisms of Storm-Time Ionospheric Response

2.1 Prompt Penetration and Disturbance Dynamo Electric Fields

During the main phase of a geomagnetic storm, the enhanced magnetospheric convection can cause a prompt penetration of interplanetary electric fields to equatorial and low latitudes (prompt penetration electric fields, PPEFs), which increases the eastward equatorial electrojet and the associated equatorial fountain effect. This drives plasma upward and poleward along magnetic field lines, producing a super-fountain effect that raises TEC at the crests of the equatorial ionization anomaly, sometimes far beyond quiet-time levels [19]. Several recent studies of the May 2024 superstorm attribute the pronounced dayside TEC enhancements over the American, Pacific, and Mexican sectors to this mechanism, with peak %dTEC timing closely tracking successive steps in the storm's main phase [17].

As the storm evolves, disturbance dynamo electric fields (DDEFs), generated by storm-enhanced thermospheric winds, become significant, typically with a delay of several hours relative to PPEF onset and often opposing it in direction [13]. DDEFs can suppress the fountain effect and contribute to negative storm phases at low latitudes even while high-latitude and mid-latitude regions remain disturbed. Multiple studies note that whether a station observes a positive or negative response, and the relative timing of the transition between the two, depends sensitively on local time of storm onset, magnetic latitude, and season [5,9].

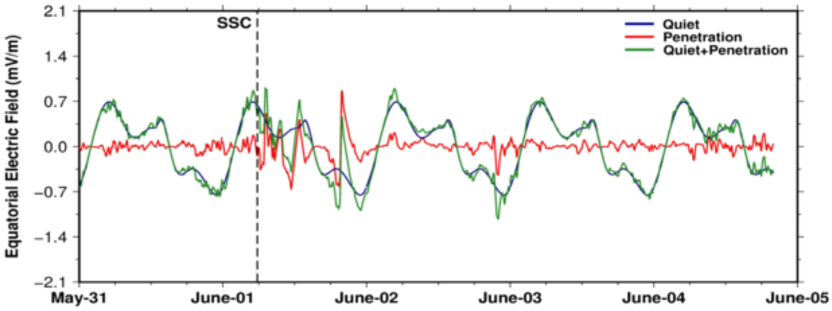

Figure 1. PPEEF model derived eastward electric fields during 31 May to 4 June [5]

2.2 Neutral Composition Changes and Negative Storm Phases

Negative ionospheric storm effects are also strongly related with variations and changes in thermospheric composition, particularly a storm-time increase in the molecular-to-atomic-oxygen ratio transported from high to low latitudes by disturbed circulation.

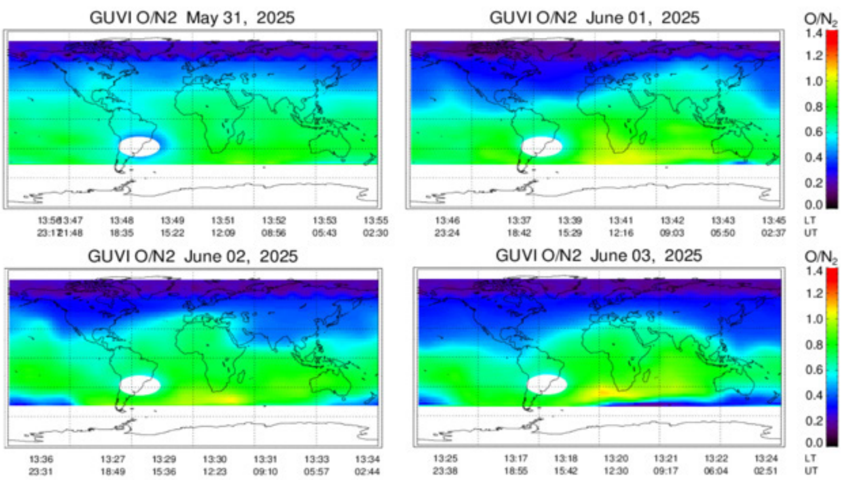

Figure 2. GUVI/TIMED satellite-derived thermosphere O/N2 during the geomagnetic storm period from 31 May to 3 June 2025 [5]

This composition change uplifts recombination rates and declines electron density, producing TEC decreases that can persist for one to several days into the storm recovery phase [5]. Reduced electron density during the main phase also weakens ionospheric conductivity and the associated current systems, including the equatorial electrojet, providing an additional diagnostic of negative storm conditions [12].

During a geomagnetic storm, neutral atmospheric composition changes specifically a reduction in the thermospheric O/N2 ratio serve as the primary driver for negative ionospheric storm phases (severe depletions in plasma density and Total Electron Content). High-latitude Joule heating during the storm causes thermal atmospheric expansion, driving an upwelling of molecular species N2 and O2 into higher altitudes where atomic oxygen O normally dominates. Powerful equator-ward neutral wind surges then transport these molecular-rich,O/N2 depleted "composition bulges" toward lower latitudes. Because atomic oxygen is essential for photoionization production O+ ions) while molecular nitrogen accelerates ion recombination loss (O+ + N2□ NO+ + N) this shift in composition drastically increases charge loss rates while reducing production, resulting in prolonged depletions of electron density across global mid-to-low latitudes during a storm's main and recovery phases.

2.3 Travelling Ionospheric Disturbances and Small-Scale Irregularities

Storm-time energy and momentum input at high latitudes launches and commences large-scale and medium-scale travelling ionospheric disturbances (TIDs) that propagate to lower latitudes and modulate TEC on time scales of tens of minutes to a few hours. During the May 2024 storm, TIDs with amplitudes on the order of 28–35 TECU were reported across both hemispheres [18]. Independently of large-scale TID structuring, storms also scale up the occurrence of smaller-scale plasma irregularities and equatorial plasma bubbles, most readily detected through ROTI, amplitude/phase scintillation indices (S4), and detrended TEC. Studies combining ROTI with continuous wavelet transform analysis have shown that storm-time irregularity occurrence is generally higher and well known by shorter dominant periodicities than during geomagnetically quiet intervals, and that ROTI and detrended TEC are typically well correlated at a given station [16].

3. TEC-Based Storm Response Studies (2023–2026)

A substantial body of recent work has focused on the 10–11 May 2024 superstorm as a reference moment. Radio-occultation-based analyses using dense COSMIC-2, Spire, and FengYun-3 sampling documented a global reduction in F-region electron density immediately after storm onset, most pronounced near the equator, together with an expansion and later merging of the electron density crests in each hemisphere, indicative of a strong storm-induced electric field response followed by wind-driven recovery [11]. During geomagnetic storms, TEC typically undergoes significant increases or decreases as energetic particles interact with the Earth's magnetosphere, leading to changes in ionization levels [7]. Complementary work using twenty low-Earth-orbit satellites reported ground-based TEC enhancements up to roughly 200 TECU and topside TEC increases of 100–155 TECU, with the largest enhancements over the Pacific and American longitudinal sectors and a pronounced expansion of the equatorial ionization anomaly toward Brazil in the dusk sector [19].

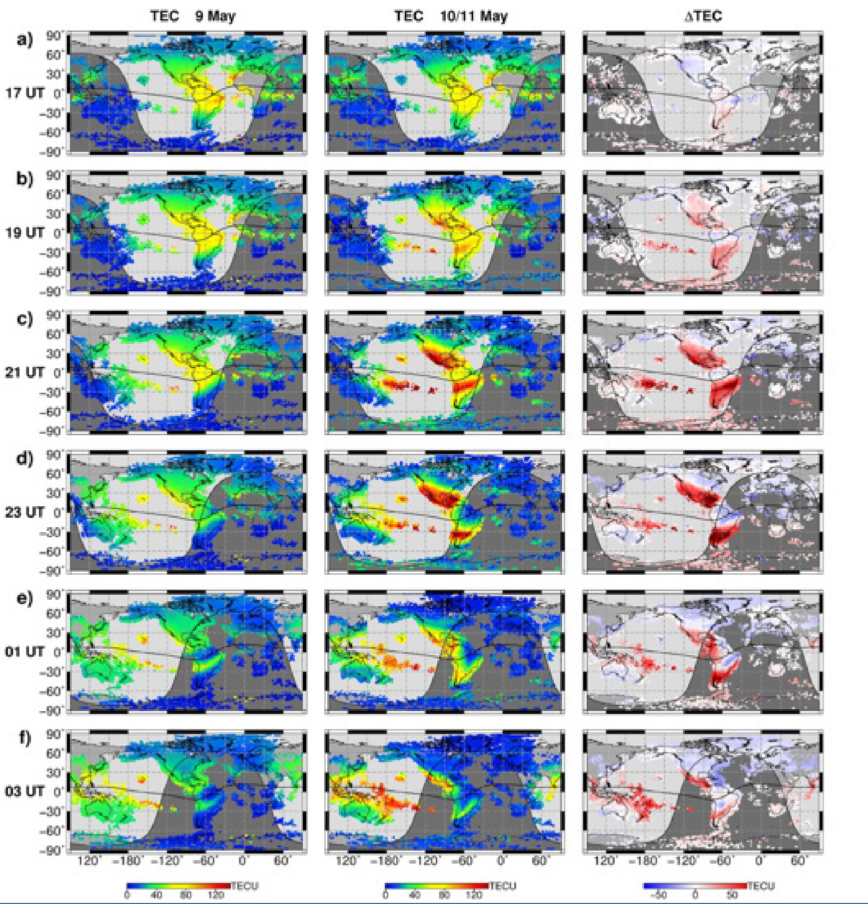

Figure 3. Ground-based GNSS TEC maps for (a–f) specific times from 17 UT to 03 UT for (left) quiet day of 9 May 2024 and (center) storm time on 10–11 May 2024, along with (right) corresponding TEC difference. The black line marks the magnetic equator, the shaded area shows terminator location and nighttime [19].

Regional case studies extend this picture. Over Ecuador, the May 2024 storm produced an approximately 30 TECU reduction in TEC during the main phase, consistent with the negative-phase, electrojet-weakening mechanism described above [12].

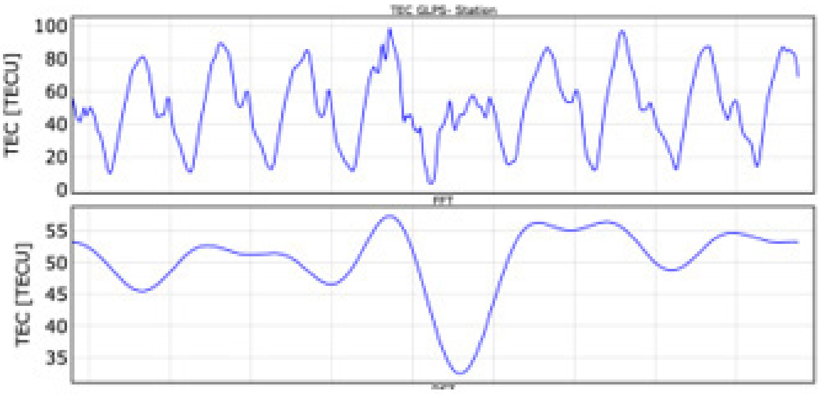

Figure 4. Variation of Total Electron Content (TEC), during the main phase of the May 2024, G5 storm [12]

Over Mexico, geodetic and low-cost GNSS receivers both captured well-defined positive and negative response phases, with %dTEC peak timing closely following successive steps in the storm's main phase, again pointing to PPEF-dominated dayside enhancement [17]. A dedicated study of the 10–12 October 2024 storm examined the EIA fountain effect in detail, showing a positive TEC response localized initially near 60°W at magnetic latitudes of ±30° that subsequently drifted westward toward 180°W at a rate much slower than the Earth's rotation, offering a rare high-resolution view of fountain-effect evolution over the storm's duration [4].

Outside the single-event literature, a study of five intense storms observed from an Indian low-latitude station over 2017–2023 used TEC, ROTI, and differential TEC together, finding that storm response character varied considerably by event: some storms enhanced ionospheric irregularities while others, such as the August 2018 event, produced a predominantly positive ionospheric response [5] A related study focused on storms near the Solar Cycle 25 peak at a low-mid-latitude Indian station reported positive responses during the main phase for some events and negative responses for others, with the sign depending on season and storm phase, and linked rapid variations in ionospheric virtual height to PPEFs using multi-instrument observations and SAMI2 modelling [9].

Collectively, these studies confirm that both the sign and magnitude of TEC storm effects are highly storm-, latitude-, and local-time-dependent [3,9,12], reinforcing the case for multi-storm statistical treatments rather than reliance on single-event case studies.

4. ROTI-Based Studies of Storm-Time Irregularities

ROTI has become a standard, low-cost proxy for ionospheric irregularity occurrence during storms, complementing amplitude and phase scintillation indices. A seven-station GNSS study of the May 2024 storm found that stations at high and sub-auroral latitudes experienced the most intense irregularities, with a strong positive correlation between ROTI and detrended TEC, and that storm-day irregularities were more pronounced and shorter-period than quiet-day irregularities [16]. A related global assessment of the same storm used ROTI dynamics to explain the pattern of GNSS precise-point-positioning errors, finding that high positioning errors coincided with large ROTI values at high latitudes, whereas mid- and low-latitude positioning degraded more gradually, a few hours after storm onset [8].

Between 2023 and 2026, ROTI (Rate of Total Electron Content Index)-based studies significantly improved understanding of storm-time ionospheric irregularities by using GNSS observations to monitor plasma density fluctuations during geomagnetic storms. Recent research showed that the occurrence and intensity of irregularities vary strongly with longitude, latitude, local time, and storm strength, with severe storms often enhancing equatorial plasma bubbles and extending irregular structures into middle latitudes. Studies of major storms during Solar Cycle 25 revealed that prompt penetration electric fields (PPEFs), disturbance dynamo electric fields (DDEFs), neutral winds, and background ionospheric conditions jointly control the development and evolution of irregularities. Multi-instrument investigations combining ROTI with satellite observations, scintillation measurements, and radio occultation data confirmed the reliability of ROTI as an indicator of large-scale plasma disturbances, although it cannot directly quantify scintillation intensity. More recently, machine-learning and forecasting models have been introduced to predict ROTI variations and improve space-weather monitoring, making ROTI an increasingly important tool for understanding and forecasting storm-time ionospheric disturbances and their impacts on GNSS systems.

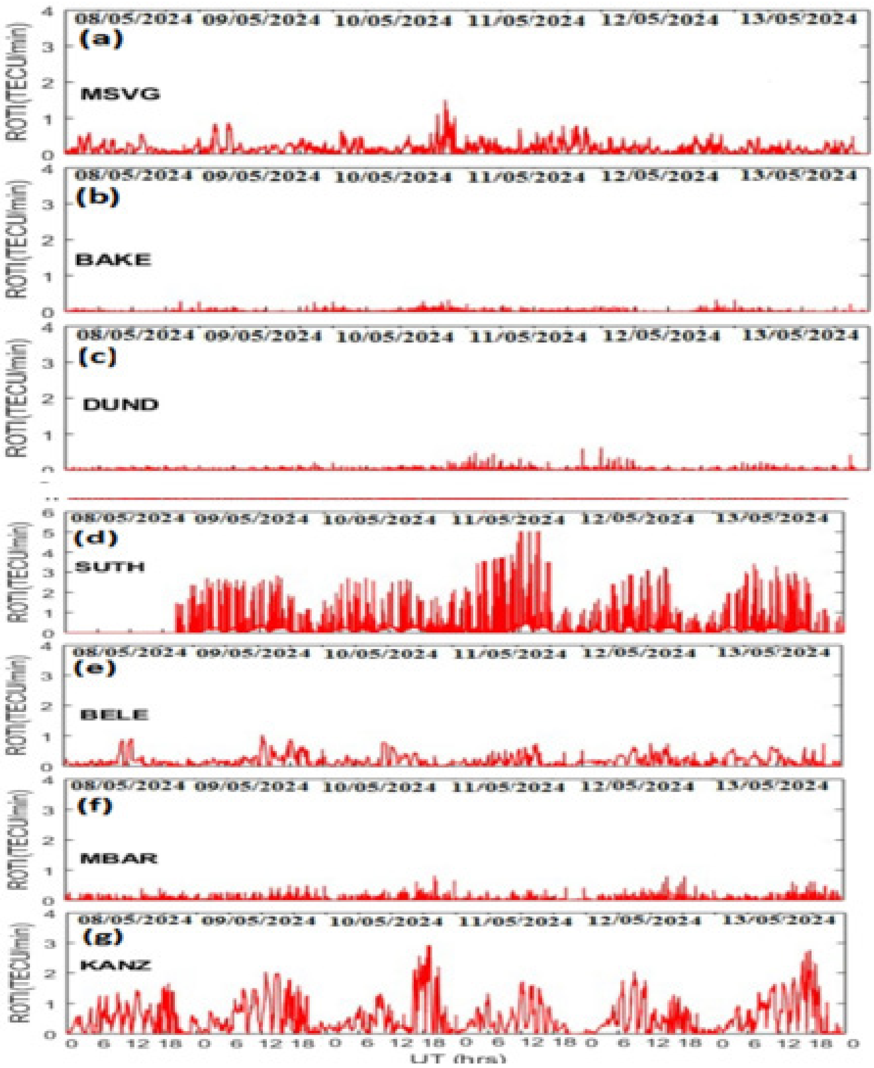

Figure 5. Rate-of-TEC Index (ROTI, in TECU/min) from 8 to 13 May 2024 at: (a) MSVG, (b) BAKE, (c) DUND, (d) SUTH, (e) BELE, (f) MBAR, (g) KANZ [16]

Methodological work has also refined how ROTI itself is computed: a study using one-second-resolution multi-GNSS data in

China showed that conventional 30-second ROTI can register spurious perturbations during non-scintillation periods, whereas 1-second ROTI tracks actual scintillation activity more reliably, a distinction demonstrated using a December 2023 storm event [20]. In the African and equatorial sector, ROTI-based studies have documented enhanced nighttime irregularities during intense storms in the eastern and western longitudinal sectors [10], and a broader climatological study linked ROTI occurrence patterns to storm drivers (coronal mass ejections versus corotating interaction regions) during the peak of Solar Cycle 24, providing a template that could be extended to Solar Cycle 25 storms [14,15]. In Southeast Asia, combined TEC and ROTI mapping during the April 2024 storm revealed the generation, eastward drift, and unusual post-midnight westward turning of equatorial plasma bubble structures, illustrating that storm-time irregularity behaviour can depart substantially from quiet-time equatorial plasma bubble climatology [1].

5. Statistical Characterization and Classification Frameworks

Despite the density of single-storm case studies produced since 2023, statistical characterization across multiple storms remains comparatively underdeveloped. Several authors have explicitly noted this gap: comprehensive investigations of CME-driven storms and their GNSS impacts remain limited, and storm classification across different solar cycle phases is incomplete because most existing studies focus on individual storm types or single events rather than a systematic multi-storm catalogue [5]. Where multi-storm statistical treatments do exist, they typically pool a handful of events (commonly three to five) selected by Dst or Kp threshold at a single station or regional network [5,9] using metrics such as peak %dTEC, storm onset-to-peak-response lag, ROTI enhancement factor relative to a quiet-time baseline, and duration of the positive or negative phase.

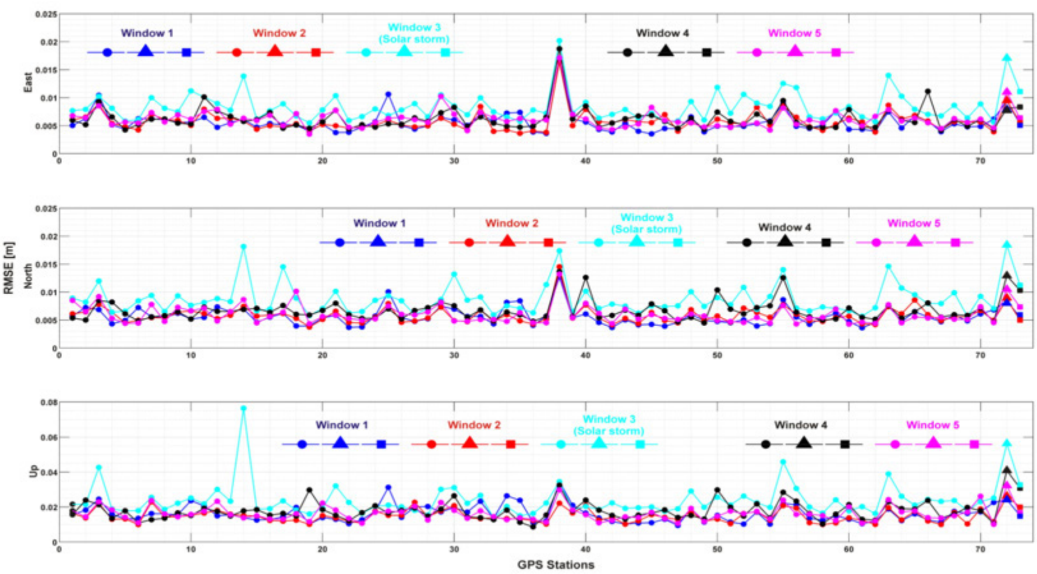

Figure 6. RMSE values of the 73 GPS stations studied. The colors represent a window of interest: blue (W1), red (W2), cyan (W3), black (W4), and pink (W5) [17]

A recurring finding across these smaller statistical studies is that storm response sign (positive versus negative) is not a fixed property of storm intensity alone; the same station can show a positive response during one storm's main phase and a negative response during another's, depending on storm onset local time, season, and the relative timing of PPEF versus DDEF dominance [5,9]. This underscores the value of a larger, multi-year statistical catalogue such as one spanning the 2023–2026 interval, which captures the ascending phase through the peak of Solar Cycle 25 and includes both moderate and extreme events (Dst below roughly −100 nT, Kp exceeding 6, up to the May 2024 superstorm) to disentangle storm-intrinsic drivers from station-specific and seasonal effects.

Table 1. Summary of results for dTEC, CWT and ROTI techniques, for the seven GNSS stations from 8 to 13 May 2024 [16]

Station	Method	8 may	9 may	10 may	11 may	12 may	13 may
MSVG	CWT periodicity	0.0313–4.0000 h	1.0000 h	4.0000 h	0.1250–3.0000 h	0.0313–4.0000 h	0.0625–3.0000 h
	Maximum ROTI	0.5 TECU/min	1 TECU/min	2 TECU/min	0.8 TECU/min	0.5 TECU/min	0.3 TECU/min
	Maximum dTEC	2 TECU	2 TECU	4 TECU	2.5 TECU	2 TECU	2 TECU
BAKE	CWT periodicity	1.0000–3.0000 h	1.0000–3.0000 h	0.0313–0.2500 h	0.0313–0.5000 h	0.0313–0.1250 h	0.2500–2.0000 h
	Maximum ROTI	0.1 TECU/min	0.2 TECU/min	0.2 TECU/min	0.2 TECU/min	0.2 TECU/min	0.2 TECU/min
	Maximum dTEC	2 TECU	2 TECU	4 TECU	4 TECU	2 TECU	2 TECU
DUND	CWT periodicity	0.2500–2.0000 h	0.1250–0.5000 h	0.0313–0.1250 h	0.0313–4.0000 h	0.0625–0.2500 h	0.2500–2.0000 h
	Maximum ROTI	0.1 TECU/min	0.1 TECU/min	0.1 TECU/min	0.2 TECU/min	0.5 TECU/min	0.2 TECU/min
	Maximum dTEC	1 TECU	1 TECU	2 TECU	4 TECU	3 TECU	3 TECU
SUTH	CWT periodicity	0.1250–0.2500 h	0.1250–5.0000 h	0.1250–5.0000 h	0.0313–4.0000 h	0.0625–0.5000 h	1.0000–4.0000 h
	Maximum ROTI	0.1 TECU/min	3 TECU/min	3TECU/min	5 TECU/min	3TECU/min	3 TECU/min
	Maximum dTEC	1 TECU	3 TECU	3.8 TECU	4 TECU	3.5 TECU	1 TEC
BELE	CWT periodicity	0.1250–0.2500 h	0.0313–2.0000 h	0.1250–0.2500 h	0.1250–0.2500 h	0.2500–2.0000 h	0.1250–0.2500 h
	Maximum ROTI	0.9 TECU/min	1 TECU/min	0.9 TECU/min	0.8 TECU/min	0.8 TECU/min	0.8 TECU/min
	Maximum dTEC	2 TECU	2 TECU	4 TECU	3 TECU	2 TECU	2 TECU
MBAR	CWT periodicity	0.1250 h	0.0625–0.2500 h	0.0625–0.5000 h	0.0625–02500 h	0.2500–0.5000 h	0.0313–0.5000 h
	Maximum ROTI	0.2 TECU/min	0.3 TECU/min	0.5 TECU/min	0.8 TECU/min	1 TECU/min	0.9 TECU/min
	Maximum dTEC	3.8 TECU	4 TECU	3.8 TECU	4 TECU	3.8 TECU	3.8 TECU
KANZ	CWT periodicity	0.0313–4.0000 h	0.0313–4.0000 h	0.1250–0.2500 h	0.1250–3.0000 h	0.0313–0.4000 h	0.0313–0.2500 h
	Maximum ROTI	1.8 TECU/min	2 TECU/min	3 TECU/min	2 TECU/min	2.5 TECU/min	3 TECU/min
	Maximum dTEC	3.8 TECU	4 TECU	3.8 TECU	4 TECU	3.8 TECU	3.8 TECU

A practical statistical framework for such a study would combine: (i) a consistent storm selection criterion (e.g., minimum Dst/SYM-H and Kp thresholds) applied uniformly across the 2023–2026 interval; (ii) station- or region-normalized %dTEC and ROTI-enhancement metrics computed relative to a quiet-time reference (e.g., a running median of the five preceding geomagnetically quiet days); (iii) classification of each storm-station pair into positive, negative, or mixed (biphasic) response categories, with response amplitude and duration recorded; and (iv) statistical association testing (e.g., correlation or contingency-table analysis) between response category and storm/geophysical parameters such as storm sudden commencement local time, season, latitude, and CME versus corotating-interaction-region storm driver. Such a framework would extend, rather than duplicate, the single-storm mechanistic studies reviewed above.

6. Regional Variability

Storm response character during 2023–2026 has shown marked regional structure. Equatorial and low-latitude American and Pacific sectors have exhibited some of the largest positive TEC enhancements on record during the May 2024 storm, driven by super-fountain effects [17,19]. African equatorial and low-latitude stations have more frequently reported enhanced nighttime irregularities and mixed positive/negative responses, with ROTI-based studies in West and East Africa documenting storm-associated irregularity enhancement across multiple longitudinal sectors [10]. Indian low- and mid-latitude stations have reported season-dependent sign reversals between main and recovery phases across several Solar Cycle 25 storms [5,9,16]. High-latitude and sub-auroral stations, in contrast, consistently show the most intense ROTI-detected irregularities and the fastest GNSS positioning degradation, reflecting direct particle precipitation and auroral electrodynamic forcing rather than the equatorial fountain-effect mechanisms dominant at low latitudes [6,16]. This regional heterogeneity is a further argument for statistical studies that stratify results by latitude and longitude sector rather than reporting only global or single-station averages.

7. Research Gaps and Future Directions

Based on the literature surveyed, several gaps need attention in future statistical characterization work. First, most multi-storm statistical studies to date cover only three to five events [5,9], which is insufficient to robustly separate storm-intrinsic from seasonal and local-time effects; a 2023–2026 catalogue would substantially increase statistical power. Second, storm classification criteria (Dst versus SYM-H versus Kp thresholds, and main-phase versus recovery-phase windowing) are applied inconsistently across studies, complicating cross-study comparison; a standardized classification scheme is needed. Third, regional data coverage remains uneven, with the African sector, the South Atlantic Anomaly, and parts of the Southern Hemisphere still comparatively under-sampled relative to North America, Europe, and East/South Asia [10]. Fourth, few studies jointly analyze TEC and ROTI within a single statistical framework, even though the two metrics capture complementary large-scale and small-scale aspects of the storm response and are shown to be correlated at individual stations [18]. Finally, the relationship between statistically characterized storm response categories and operational GNSS positioning degradation has been explored mainly through single-event case studies [6, 18]; linking a multi-storm statistical TEC/ROTI catalogue directly to positioning error statistics would strengthen the applied relevance of future work.

8. Conclusion

The period 2023-2026 has seen an extraordinary sequence of intense and extreme geomagnetic storms during the rising and maximum phases of Solar Cycle 25. The literature on positive and negative ionospheric storm effects and storm-time irregularities. TEC-based studies consistently show that the sign and magnitude of storm response are determined by the interplay between prompt penetration and disturbance dynamo electric fields, neutral composition changes and travelling ionospheric disturbances, which are modulated by latitude, local time and season. ROTI-based studies confirm that storm-time irregularity occurrence is enhanced relative to quiet conditions and correlates with detrended TEC, with the strongest effects at high and equatorial latitudes. However, statistical characterization pooling multiple storms across full solar cycle phases remains limited, with inconsistent classification criteria and uneven regional coverage. To fill this gap, a dedicated statistical study based on the 2023–2026 storm catalogue, including normalized TEC and ROTI metrics with a standardized storm classification scheme across multiple latitudinal sectors, would provide a more robust empirical basis for both physical interpretation and operational space weather forecasting.

Conflict of Interest

The authors declare that they have no known competing financial interests or personal relationships that could have appeared to influence the work reported in this manuscript.

References

1. Abadi P, Muafiry IN, Pratama TN, Putra AY, Faturahman A, et al. (2025) Post-Sunrise Ionospheric Irregularities in Southeast Asia During the Geomagnetic Storm on 19–20 April 2024. Remote Sensing 17: 2906.

2. Agago TT, Terefe DA, Gebino GK (2025) Ionospheric storm effects during the 5–6 November 2023 geomagnetic storm over South Africa. Geomagnetism and Aeronomy 65: 132-145.

3. Astafyeva E, Yasyukevich YV, Maletckii B, Oinats A, Vesnin A, et al. (2022) Ionospheric disturbances and irregularities during the 25–26 August 2018 geomagnetic storm. Journal of Geophysical Research: Space Physics 127: e2021JA029843.

4. Bojilova R, Mukhtarov P, Pancheva D (2024) Global ionospheric response during extreme geomagnetic storm in May 2024. Remote Sensing 16: 4046.

5. Chougule P, Shetti D, Venkatesh K, Seemala GK, Chougule S (2025) A study of the ionospheric response during intense geomagnetic storms over the Indian low-latitude region during the period 2017–2023. Advances in Space Research.

6. Danilchuk E, Yasyukevich Y, Vesnin A, Klyusilov A, Zhang B (2025) Impact of the May 2024 extreme geomagnetic storm on the ionosphere and GNSS positioning. Remote Sensing 17: 1492.

7. Data EA, Terefe DA, Gutulo SG, Teklemariam AL, Gebino GK, et al. (2026) Dynamics of equatorial and low-latitude TEC fluctuations during the April 2023 geomagnetic storm. Kinematics and Physics of Celestial Bodies 42: 24-39.

8. Gonzalez WD, Joselyn JA, Kamide Y, Kroehl HW, Rostoker G, et al. (1994) What is a geomagnetic storm? Journal of Geophysical Research: Space Physics 99: 5771-5792.

9. Gupta A, Ahmed Q, Singh A, Rawat A, Bhardwaj A, et al. (2025) Ionospheric response of intense geomagnetic storms near the peak phase of solar cycle 25 at low mid-latitude Indian station, New Delhi. Advances in Space Research.

10. Kassa Y, Tebabal A, Damtie B (2024) Nighttime ionospheric irregularity during intense geomagnetic storm events over the Europe-African longitudinal sector. Heliyon 10.

11. Lee W, Liu G, Wu DL, Rowland DE (2025) Ionospheric response to the 10 May 2024 geomagnetic storm as observed in GNSS radio occultation electron density. Journal of Geophysical Research: Space Physics 130: e2024JA033489.

12. López ED, Barbier H, Carvajal W, Guamán L (2025) Ionospheric Response to the May 11, 2024, Geomagnetic Superstorm over Ecuador. arXiv.

13. Mukhtarov P, Bojilova R (2025) Low-Latitude Ionospheric Anomalies During Geomagnetic Storm on 10–12 October 2024. Universe 11: 295.

14. Oliveira DM, Piersanti M, Walach MT, Alves LR, Tobiska WK, et al. (2025) Impacts of the extreme Gannon geomagnetic storm of May 2024 throughout the magnetosphere-ionosphere-thermosphere system. Frontiers in Astronomy and Space Sciences 12: 1742847.

15. Ondede GO, Rabiu AB, Okoh D, Baki P, Olwendo J, et al. (2022) Relationship between geomagnetic storms and occurrence of ionospheric irregularities in the west sector of Africa during the peak of the 24th solar cycle. Frontiers in Astronomy and Space Sciences 9: 969235.

16. Uluma E, Lomotey SO, Bankole FJ, Nguessan K, Muniafu W, et al. (2026) Investigation of ionospheric irregularities during the severe geomagnetic storm of 10–11 May 2024. Indian Journal of Physics 100: 1-19.

17. Vazquez-Ontiveros JR, Melgarejo-Morales A, Martinez-Felix CA, Martinez-Batlle JR (2025) Analysis of ionospheric response and GNSS positioning on geodetic and low-cost receivers in Mexico during the May 2024 geomagnetic storm. Geosciences 15: 408.

18. Yang Z, Morton YTJ (2025) Impacts of the May 2024 extreme geomagnetic storm on global high-accuracy GPS positioning solutions. Space Weather 23: e2025SW004547.

19. Zakharenkova I, Cherniak I, Braun JJ, Weiss JP, Wu Q, et al. (2025) Unveiling ionospheric response to the May 2024 superstorm with low-Earth-orbit satellite observations. Space Weather 23: e2024SW004245.

20. Zhang Z, Wang N, Liu A, Li Z, Li A, et al. (2025) Assessing 1-second ROTI for ionospheric perturbation monitoring using real-time multi-GNSS data in China. Space Weather 23: e2024SW004187.